Check for updates

Textile Research Journal

Original article

Textile Research Journal
0(00) 1–13
© The Author(s) 2020
Article reuse guidelines:
sagepub.com/journals-permissions
DOI: 10.1177/0040517520935984
journals.sagepub.com/home/trj
SAGE

Fabric defect detection based on a deep convolutional neural network using a two-stage strategy

Xiang Jun, Jingan Wang, Jian Zhou, Shuo Meng, Ruru Pan and Weidong Gao

Abstract

With the rise of labor costs and the advancement of automation in the textile industry, fabric defect detection has become a hot research field in recent years. We proposed a learning-based framework for automatic detection of fabric defects. Firstly, we use a fixed-size square slider to crop the original image to a certain step and regularity. Then an improved histogram equalization is used to enhance each cropped image. Furthermore, the Inception-V1 model is employed to predict the existence of defects in the local area. Finally, we apply the LeNet-5 model, which plays the role of a voting model, to recognize the type of the defect in the fabric. In brief, the proposed framework mainly consists of two steps, namely local defect prediction and global defect recognition. Experiments on the dataset have demonstrated the superior performance in fabric defect detection.

Keywords

fabric defect detection, feature extraction, convolutional neural network, object detection, image analysis

The advent of fabric defects impair fabric quality, appearance and properties and consequently diminish the profit of manufacturers, so the detection of fabric defects is a vital procedure during the textile corporations' quality control work. The presence of defects in the fabric can reduce prices with losses reaching 45–60%. Traditionally, fabric inspection is accomplished by human visual checking, which suffers from low efficiency and high labor cost. Moreover, manual inspection results are also unreliable due to recognition errors caused by fatigue and the fact that some inconspicuous and small defects are difficult to check for. Thus, human fabric defect detection is already unsuitable for modern textile manufacture. Replacing manual detection with a computer vision-based detection is an inevitable trend of automation and informatization for the textile industry. While researches on automatic fabric inspection[1–6] have been done over 30 years, there is no widely available type of automated fabric inspection machine, which is essentially caused by a lack of adaptivity in the existing algorithms on various types of defects. The detection algorithm is the key to the automatic fabric inspection machine.

Applications of artificial intelligence techniques can offer a low-cost and high-efficiency for decision-making in many domains. Consequently, advanced detection technologies, which can be integrated into the existing fabric inspection machine, are in increasing demand. Moreover, with the continued development of the textile industry, the texture of fabric has become more and more complex and diverse. With the improvement of waving technology, inconspicuous and small defects in fabric have become more and more common, which makes the detection task more challenging. Consequently, the research of developing a robust model with high accuracy and efficiency for defect detection has great significance. This paper proposes a

Key Laboratory of Eco-textiles, Ministry of Education, Jiangnan University, China

Corresponding author:
Weidong Gao, Jiangnan University, Lihu Road, 1800 Wuxi, Jiangsu 214122, China.
Email: gaowd3@163.com

novel framework for fabric defect detection-based convolutional neural networks (CNNs)[7] using a two-stage strategy.

The yarn in the fabric is highly regularly aligned, resulting in a high periodicity of sub-patterns of the fabric. The appearance of defects breaks the periodicity of the fabric. According to the directional characteristics, these defects can be divided into three groups: (1) defects in the weft direction; (2) defects in the warp direction; (3) defects without directional features. From the view of computer vision, the fabric defects are considered as anomalous arrayed pixels in the image compared with the non-defect areas. The purpose of automatic defect detection is to detect the types and the locations of any possible defects without any human interventions. The performances of defect detection algorithms are generally evaluated by three criteria: (1) the detection rate, which represents the sensitivity of the detection model; (2) the false alarm rate, which reflects the robustness of the model; (3) model efficiency, which denotes the feasibility of the detection model for industrial application.

At present, most of the defect detection methods employ an offline method, which means that the fabric defects are detected after it is taken off the loom. These methods generally enable batch inspection of fabrics with faster speeds. However, their detection accuracy is low and the cost is high. To avoid these disadvantages, this study proposes an online defect inspection system, which contains two modules: a hardware system and a software system (the detection algorithm framework is the system core). The main function of the hardware system is to collect images in real time and transmit them to an external computer. The software system is only responsible for identifying the image defect information and feeding it back to the production workers. When a defect is found, the equipment can promptly notify the production personnel to deal with it. The hardware system is shown in Figure 1. This paper mainly introduces the proposed detection algorithm framework.

Inspired by the research advancement in deep learning,[8–14] a framework based on this technology is proposed for plain fabric defect detection in this study. The framework consists of two stages: local defect prediction and global defect recognition. The training of the two models is based on supervised learning. The rest of this paper is organized as follows. Related works are reviewed in the second section. The third section introduces the key technologies in the framework. The fourth section describes the dataset and presents an extensive evaluation and comparison, in addition to the component analysis of the proposed method. The fifth section concludes the paper.

Related work

Since the 1980s, researchers have proposed many different detection models for fabric defects. According to different image analysis methods in their models, the models can be divided into four categories: statistics-based methods, spectrum-based methods, model-based methods and learning-based methods.

The statistical-based methods are realized by analyzing the spatial distribution of pixel gray values and then extracting the feature values. An important assumption is that the defectless area of the fabric surface has stable statistical characteristics, and the appearance of defects will destroy this stability. Statistical-based methods trend to distinguish defects through feature analysis of standard textiles. The methods generally divide the test image into image blocks. A long time ago, many researchers focused on such methods based on first-order statistics (such as means and variances) or second-statistics (such as co-occurrence matrices and auto-correlation functions).[15–18] However, the limitation of these methods is that it is very difficult to discriminate blurry and small defects that do not change the average grayscale of a fabric image. Recently, Zhang et al.[19] proposed a novel fabric defect approach based on the saliency metric for color dissimilarity and positional aggregation. This method performs well for detecting significant defects, but it is not sensitive to small defects.

Since the fabric texture has a regular periodicity, the fabric image can be detected in the frequency domain by time–frequency conversion. In spectrum-based methods, regarding yarns as basic texture primitives, a texture pattern can be extracted by analyzing the frequency spectrum of fabric sample images. Chan and Pang[5] defined a Fourier spectrum-based model, called the central spatial frequency spectrum, to extract seven eigenvalues for fabric defect detection. Due to the difficulty in quantifying the contribution of each spectral component of the infinite Fourier basis, Fourier analysis is only suitable for detecting large and obvious defects. Lambert and Bock[20] applied wavelet optimal basis decomposition to divide the fabric image into three layers, then composed the wavelet coefficients in each layer into one feature vector. Finally, the feature vector is used as the input of a neural network to identify and locate the defect. Bodnarova et al.[21] employed an optimized Gabor filter generation method to detect defects in fabric images and obtained a good performance on their dataset. Although wavelet transform, which consists of small waves of varying frequency and limited duration, is useful for detecting small defects, its redundant and massive computational cost would greatly affect the work efficiency in real industry. Jia et al.[22] presented an automatic defect inspection

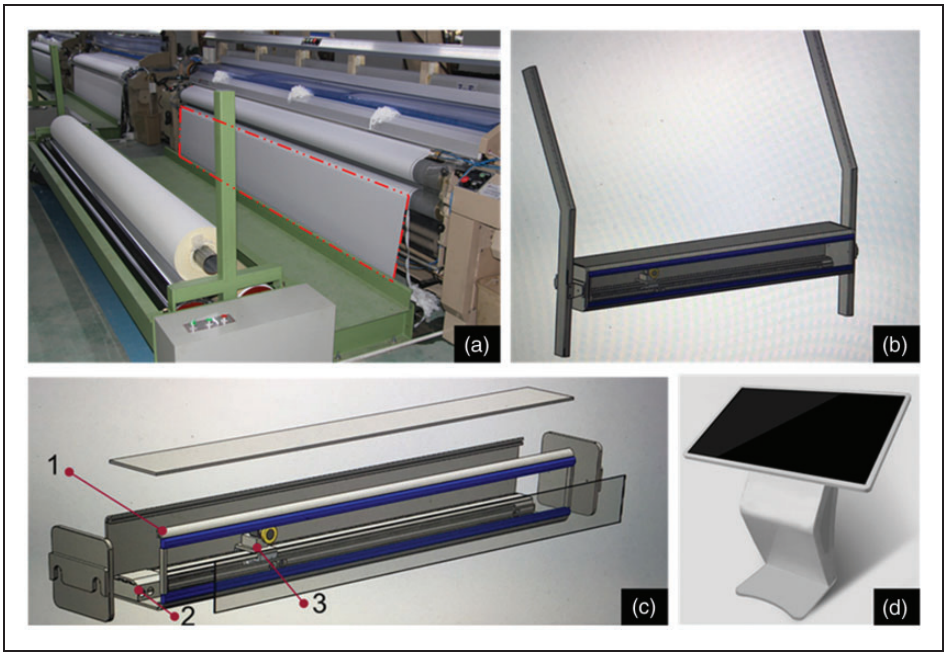

Figure 1. Online defect detection device: (a) a common loom; (b) detection device schematic (installed in the red dashed box position on the left in (a)); (c) detection device detail: 1 – embedded control mechanism, 2 – horizontal rail, 3 – camera and light source; (d) external computer. (Color online only.).

approach that is based on lattice segmentation and Gabor filtering. Although this method avoids the above disadvantages to a certain extent, it is still only applicable to some obvious defects.

The model-based methods represent fabric texture as a stochastic process and hold the hypothesis that the texture image can be regarded as a sample that is generated by the stochastic process in the image space. Defect detection is treated as a hypothesis test problem of statistical information derived from this model. Representative models in this field mainly include the Gauss–Markov random field (GMRF)[23] model and Gaussian mixture model.[24] These methods are usually computationally expensive, and their detection accuracy of small defects cannot meet the requirement.

In the early learning-based defect detection methods, artificial neural networks were generally used to identify and classify extracted features. Kumar[25] proposed a feedforward neural network that uses the variance eigenvalues extracted by singular value decomposition principal component analysis as input to detect the fabric image. Kuo et al.[26] used a three-layer backpropagation neural network to perform online detection of fabric images captured by a 4096-pixel line array camera. The method achieved a detection rate of 91.88 on the dataset with 160 images. The idea of these methods is to first extract the features of the fabric image and then classify the features using a neural network. This leads to the detection method being heavily dependent on the feature extraction algorithm, which makes the methods less robust.

Recently, significant progress has been made on image analysis by moving from low feature-based algorithms to deep learning-based end-to-end frameworks. Many researchers are committed to solving fabric defect detection problems with deep learning techniques. Tong et al.[27] presented a non-locally centralized sparse representation model, which is based on the learned sub-dictionaries. Ouyang et al.[28] developed a deep learning-based algorithm for an on-loom fabric defect inspection system by combining the techniques of pre-processing, fabric motif determination, candidate defect map generation and CNNs. Li et al.[29] proposed a novel fabric defection method based on biological vision modeling. The key technologies include fabric image representation, low-rank representation model construction, model optimization and saliency map generation and segmentation. These methods all perform well on the TILDA dataset, and the detection rate is high for obvious defects. However, there are several cases where these methods do not provide accurate defect identification: (1) the defects in the image are small (the length and width of the area where the defect is located are no greater than 10 pixels); (2) there are both defects and folds in the image. The first step of the proposed method uses a small slider to scan the entire image, so that small defects can be detected. In addition, by adding fabric samples with folds in the

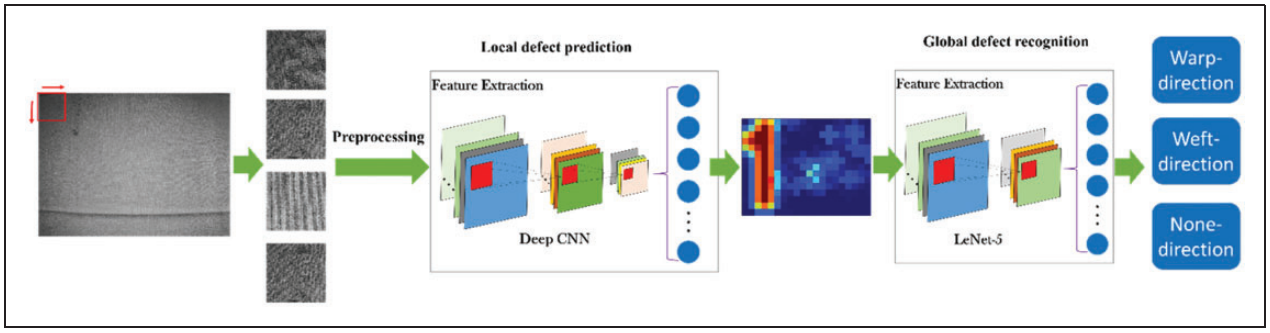

Figure 2. Framework of the proposed fabric defect detection method. CNN: convolutional neural network.

training set, the generalization performance of the model is increased, so that the model can distinguish between folds and defects.

Detection algorithm

The proposed method aims at developing a principled methodology ensuring full automation of defect detection while enabling it to efficiently cope with several types of fabrics and defects. As shown in Figure 2, our approach is composed of three components, namely image pre-processing, defect prediction and defect recognition. In the first step, pre-processing is used to make the defect in the image appear more clearly. The second step is mainly to judge whether there is a defect in the box-image. This step also involves training a deep CNN to predict the possibility of defects. In the third and final step, by analyzing the data extracted in the previous step, the defects in the image are located and roughly identified. In what follows, we give details about each of the above steps separately.

Pre-processing of fabric images

To make our approach generalizable to types of defects and multiple fabric groups, we first use a fixed-size square slider to crop the original image to a certain step and regularity. In this paper, we use a square slider with the size of 224×224. To enhance the contrast of the image without causing intensity saturation and detail corrosion, this paper applies a histogram equalization (HE) method for effective and efficient mean brightness preservation and contrast enhancement. The method first separates the histogram of the input image into two sub-histograms. Then the sub-histograms are modified by the plateau limits, which are calculated from the respective sub-histograms. Finally, HE is performed on the modified sub-histograms respectively. The method of image enhancement consists of three main steps: histogram segmentation, histogram modification and histogram transformation.

For the histogram segmentation, we first find the separating point (SP) (i.e., the mean intensity of the original histogram), which can be represented by

$$SP = \frac{\sum_{k=0}^{L-1} l_k \times n_k}{N} \tag{1}$$

where n_k is the number of pixels in the image with the gray level l_k, N is the total number of pixels in the input image and L is the max-range of the gray level. Then, by applying this value, the histogram of the original image is separated into two sub-histograms, the low sub-histogram (represented by $HISL$) and high sub-histogram (represented by $HISH$).

After histogram segmentation, the plateau limits of both sub-histograms are computed. Here we set three plateau limits in each sub-histogram for a total of six. The plateau limits (PL) can be calculated by

$$PL = GR \times Pk \tag{2}$$

where GR is the gray level ratios, whose values ranges from 0 to 1, and Pk is the peak value of the input histogram. For the proposed method, there are three peak coefficients in each sub-histogram. The GR values in each sub-histogram are defined as

$$GR_{L1} = GR_{L2} - D_L \tag{3}$$

$$GR_{L2} = \frac{SP - SP_L}{SP - L_{\min}} \tag{4}$$

$$GR_{L3} = GR_{L2} + D_L \tag{5}$$

$$GR_{H1} = GR_{H2} - D_H \tag{6}$$

$$GR_{H2} = \frac{L_{\max} - SP_H}{L_{\max} - SP} \tag{7}$$

$$GR_{H3} = GR_{H2} + D_H \tag{8}$$

$$D = \begin{cases} \frac{1-GR_2}{2} & GR_2 > 0.5 \\ \frac{GR_2}{2} & GR_2 \le 0.5 \end{cases} \quad (9)$$

where SP_L and SP_H represent the separating point in each sub-histogram, D represents the gray level ratio differences in each sub-histogram and $L_{\max}$ and $L_{\min}$ are the max-gray value and min-gray value, respectively, in the histogram. Figure 3 shows the calculated plateau limits for each sub-histogram. Then, the histogram modification is applied on the original histogram based on the obtained plateau limits. As also shown in Figure 3, the non-zero bins that are lower or equal to the first PL are clipped to PL_1. The bins between PL_1 and PL_3 are clipped to PL_2. Bins greater than PL_3 are limited to PL_3. These clipping processes can avoid the intensity saturation problem.

Finally, we apply the histogram transformation into the modified sub-histogram by using the conventional HE. However, the probability density function (PDF) and cumulative density function (CDF) for each modified sub-histogram need to be calculated. Finally, the enhancement process for the input image can be described as

$$T(k) = \begin{cases} SP \times CDF_L(k) & k \in [l_{\min}, SP] \\ SP + 1 + (255 - SP - 1) \times CDF_H(k) & k \in (SP, l_{\max}] \end{cases} \quad (10)$$

Local defect prediction

Significant progress has been made on image recognition by moving from the early low-level feature-based algorithms to deep learning-based frameworks. Inspired by the advancement of deep learning, this approach applies a sparse CNN using an Inception module[30] to predict the possibility of defects in the image. The main design idea of the Inception architecture is to find a locally optimal sparse structure in a CNN. This structure needs to be covered and approximated by dense components that can be obtained. The modules used in the proposed framework are shown in Figure 4. In each module, 1×1 convolutions are used to reduce the input dimension of before 3×3 convolutions. In addition to dimensionality reduction, they are also used for data rectified linear activation, which makes it a dual mission.

Considering the computational cost, the proposed method uses the grayscale image as the input of the detection framework. After the image enhancement, the box-image is still a grayscale image with the size of 224×224. However, the input size of the original Inception-V1 network is $224 \times 224 \times 3$ (color image). Therefore, we make some modifications based on the original network. Szegedy et al.[31] proposed four principles that generally need to be followed when designing neural networks: (1) avoid representational bottlenecks; (2) higher-dimensional representations are easier to localize in the network; (3) spatial aggregation can be done on lower-dimensional embedding without causing any or all loss in presentation capabilities; (4) balance the width and depth of the network. According to these principles, the network architecture in this step is described in Table 1.

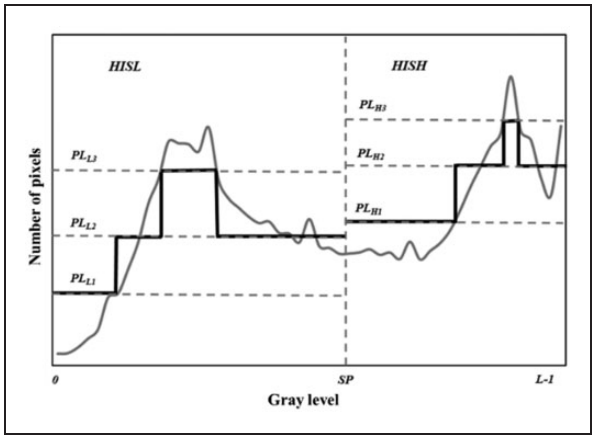

Figure 3. Histogram with three plateau limits set.

Early in the network, four convolutional layers and two pooled layers were used to change the input size from $224 \times 224 \times 1$ to $28 \times 28 \times 192$. In order to avoid representational bottlenecks, the size of the convolution kernel is all 3×3 instead of the commonly used 7×7 and 5×5. Immediately following the Inception part of the network, the two Inception structures shown in Figure 4 are used, where Inception module 1 is mainly used to increase the network sparseness and Inception module 2 is used to increase the sparsity while reducing the grid size. The latter part is the common structure of the convolutional network. The output size of the network inception section is $7 \times 7 \times 2048$. Then we use a 7×7 pooled layer and a 1×1 convolution layer to reduce the dimension of the feature and integrate the feature vectors. A dropout layer with 40% ratio of dropped outputs is used to prevent overfitting. At the end of the network, we use a linear layer with softmax loss as the classifier.

Global defect recognition

After all box-images have been predicted, we can obtain a feature map for the input image. Then a simple CNN is applied to recognize the defect type based on the feature map with a size of 32×24. Firstly, the feature map is normalized into a square of size 32×32, by way of zero padding. The proposed method applies Lenet-5 to recognize the feature map.

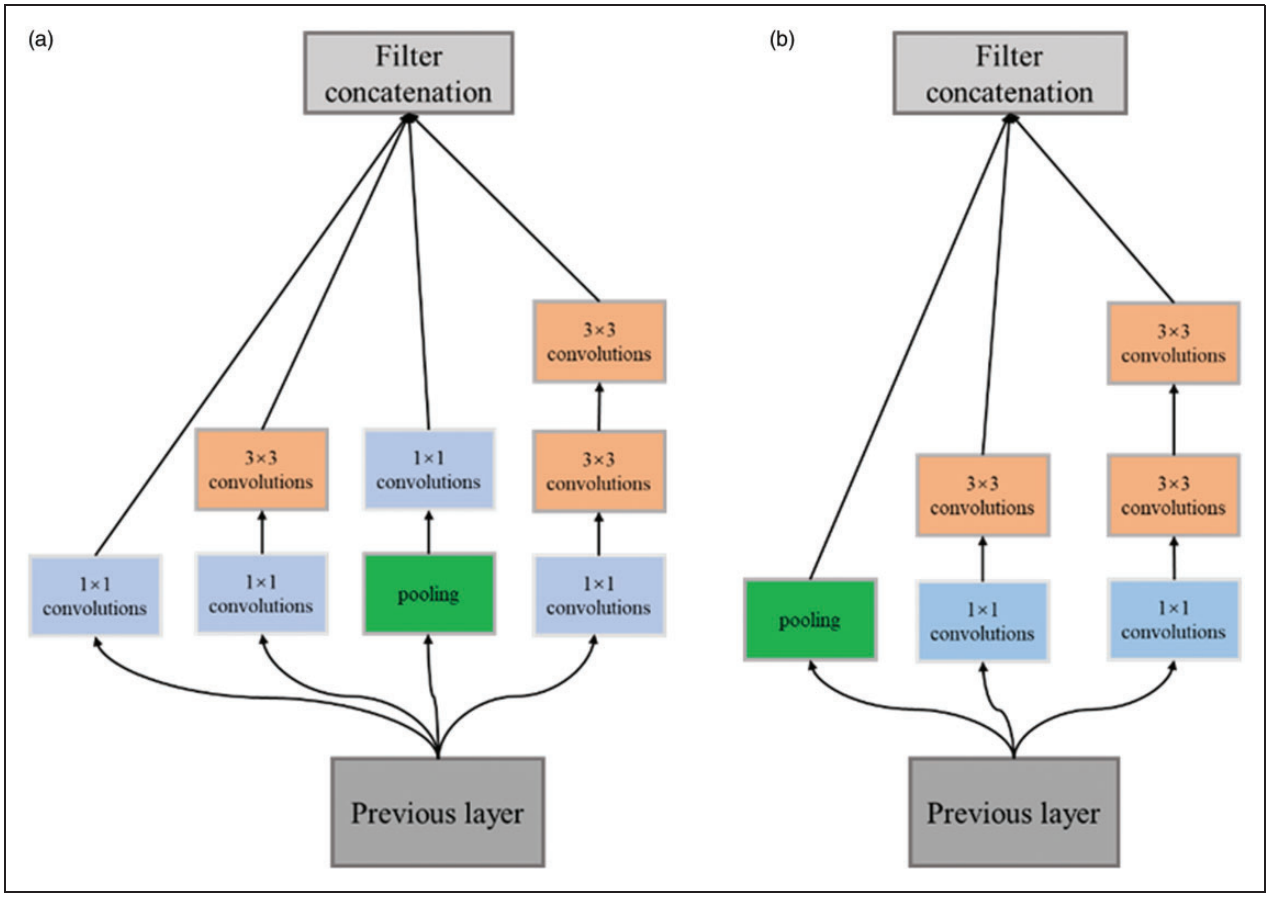

Figure 4. The two Inception modules used in the proposed framework: (a) Inception module 1; (b) Inception module 2.

Table 1. Outline of the convolutional neural network architecture

Type	Patch size/stride	Output size
Convolution	$3 \times 3/1$	$224 \times 224 \times 64$
Pool	$3 \times 3/2$	$112 \times 112 \times 64$
Convolution	$3 \times 3/1$	$112 \times 112 \times 96$
Convolution	$3 \times 3/2$	$56 \times 56 \times 192$
Pool	$3 \times 3/2$	$28 \times 28 \times 192$
Inception $\times$ 2	Inception module 1	$28 \times 28 \times 320$
Inception	Inception module 2	$14 \times 14 \times 576$
Inception $\times$ 4	Inception module 1	$14 \times 14 \times 786$
Inception	Inception module 2	$7 \times 7 \times 1280$
Inception $\times$ 2	Inception module 1	$7 \times 7 \times 2048$
Pool	7×7	$1 \times 1 \times 2048$
Convolution	1×1	$1 \times 1 \times 1000$
Dropout	40%	$1 \times 1 \times 1000$
Linear	Logits	$1 \times 1 \times 1000$
Softmax	Classifier	2

The architecture of the network is shown in Figure 5. The network includes seven layers, consisting of three convolution layers, two pooling layers and two fully connected layers. The kernels of the three convolution layers (C1, C3, C5) are all 5×5, and both pooling layers have a window size of 2×2. We use Relu as its activation function. The main function of the fully connected layer connected to the last convolutional layer is the fusion and enhancement of features. Finally, a softmax classifier is applied for category prediction.

Experimental details

Dataset and implementation

To the best of our knowledge, TILDA is a dataset specially used for defect detection. However, due to the limitation of the number of samples and the collection conditions, this dataset is not suitable for the proposed model. Due to the potential value of fabric defect detection in many applications, we created a dataset for this work. This dataset contains 2000 images with defects and 3000 images without defects, most of which come

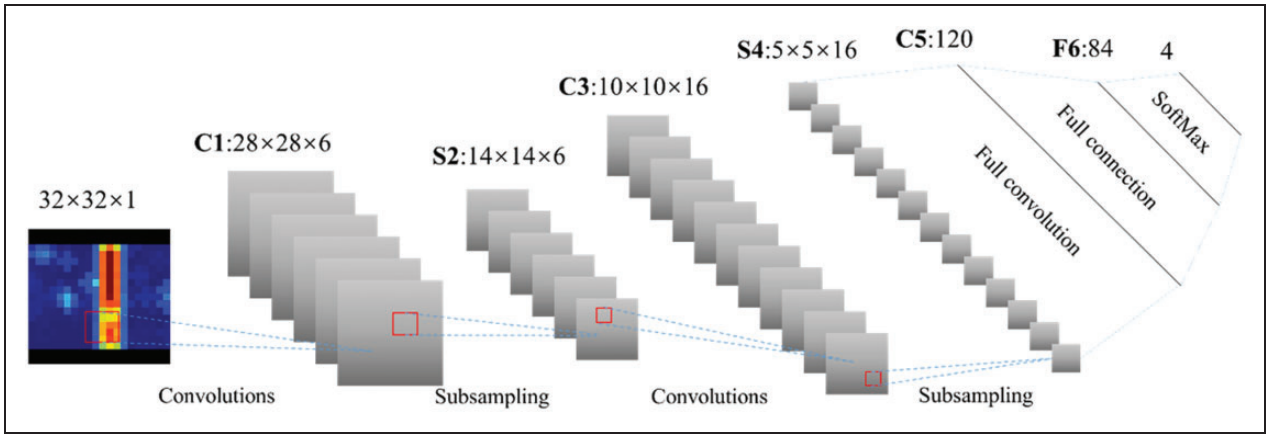

Figure 5. The structure of the global defect recognition model.

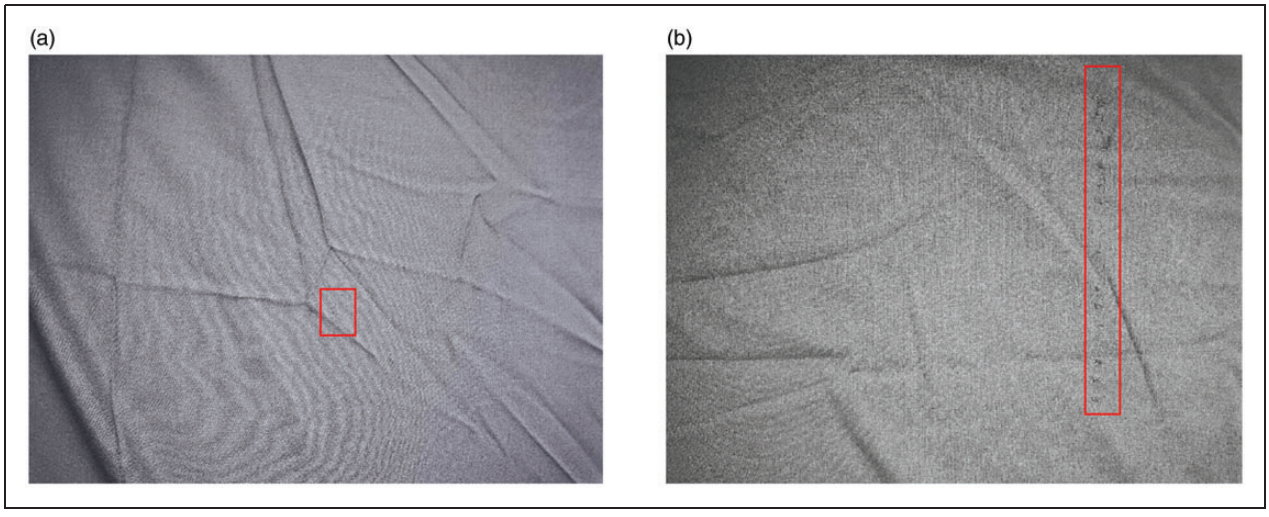

Figure 6. Two sample images with defects in the dataset: (a) a fabric image with a small defect (Reed Misdraw); (b) a fabric image with an obvious defect (Clip Mark).

from the Tianchi competition (https://tianchi.aliyun.com/competition/entrance/231666/information). Moreover, the images with defects are classified into three categories. The size of all images is 2560×1920. To enhance the generalization of the data, we deliberately produced some artificial folds on the fabric surface, as shown in Figure 6. To train the local defect prediction model, we crop the original image with a frame of size 224×224, where the area containing the defect is a positive sample and the area without the defect is a negative sample. What we need to state here is that the negative sample dataset comes not only from normal images, but also from the innocent parts of the images with defects. Through this approach, we get a dataset for training with about 200,000 images. For the training of the global recognition model, we use the feature maps resulting from the local defect prediction model as its training set.

We train the two CNN models to utilize the deep learning framework named Tensorflow. The hardware environment of the training is an HP workstation (Z840 TOWER: CPU-E5-2623 V4@2.63GHz, Memory 32G) with a NVIDIA TITAN XP GPU (11G graphics memory).

Training for the local defect prediction model. During the training, we first initialize the model using random initialization. The learning rate initial value is set to 1e-4, and it attenuates 0.04 every four epochs. To avoid overfitting, we set the hyper-parameter weight-decay of the CNN to 1e-6. Moreover, an ADAM optimizer is

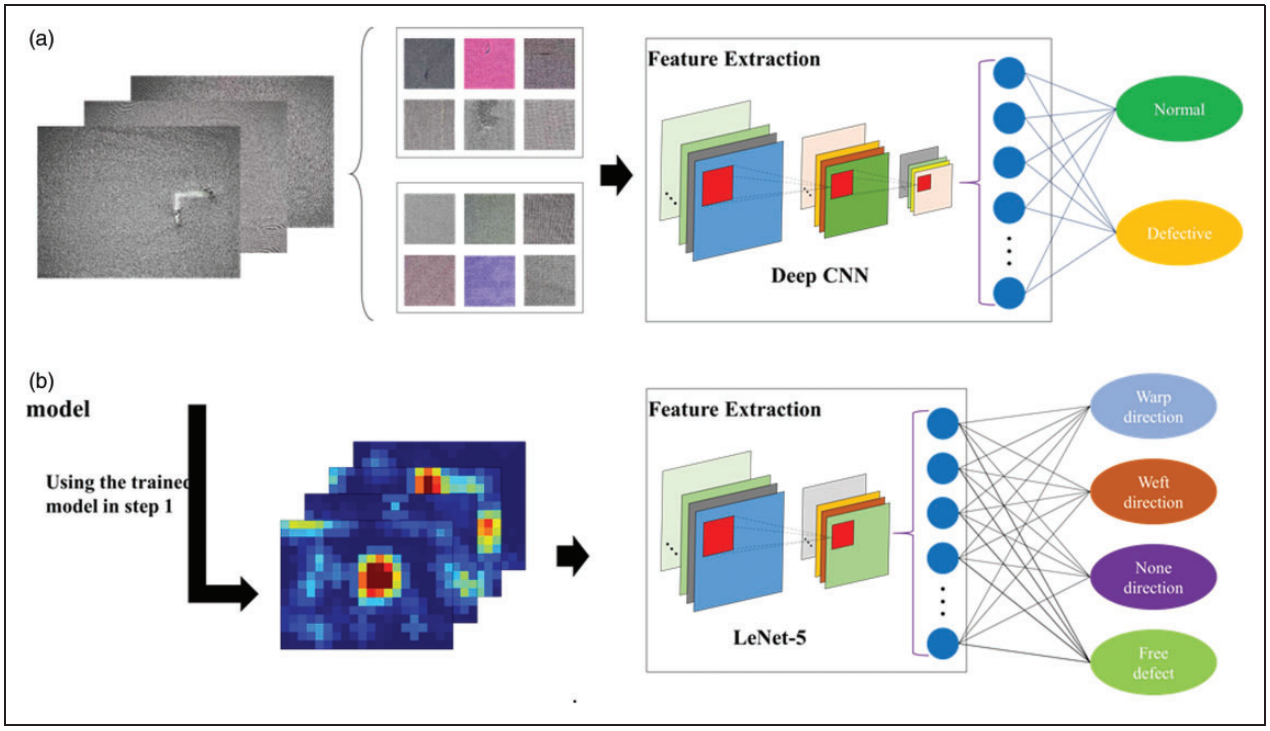

Figure 7. The architecture of the proposed defect detection system. CNN: convolutional neural network.

applied to optimize the model. We use Relu as the activation function. After the activation, batch normalization is employed to speed up the training and avoid the gradient disappearing and explosion. The function of this trained model is to predict the possibility of defects in the input box-image.

Training for the global defect recognition model. The training dataset is obtained by using the trained model in Step 1. Actually, the input of this model is the feature map of the original fabric image. During the training, we use SGD (Stochastic Gradient Descent) to optimize the model. The learning rate is fixed at 0.01. The batch size is 32.

As shown in Figure 7, when given a fabric image, first we need to use a box of 224×224 to crop the original image according to a fixed step size and regularity. This slider will move 32 steps in the horizontal direction and 24 steps in the vertical direction. After the cropping, we can get $32 \times 24 = 768$ box-images from the original image. To increase the degree of discrimination, each box-image needs to be enhanced by using the approach presented previously. Then, these box-images are divided into 12 batches (the batch size is 64) and entered into the local defect prediction model. After that, we can get a feature map, which can represent the distribution of defects in the original image. By identifying this feature map using the global defect recognition model, we can be informed whether there are defects in the original image and the types of defects.

Evaluation metrics

In this study, we use the following four evaluation metrics to appraise the performance of defect detection models. The evaluation metrics are detection rates (D_R), false alarm rates (F_R), area under the curve (AUC) and detection success rates (also known as detection accuracy and called D_{ACC}), all of which are expressed as percentages. Their definitions are as follows

$$D_R = \frac{TP}{M} \tag{11}$$

$$F_R = \frac{FP}{N} \tag{12}$$

$$AUC = \frac{\sum_{i \in positive} rank_i - \frac{M \times (M+1)}{2}}{M \times N} \tag{13}$$

$$D_{ACC} = \frac{TP + TN}{FP + FN + TN + FP} \tag{14}$$

where M and N respectively denote the total number of defect and defect-free images. The definitions of TP,

FP, *FN* and *TN* can be seen in Table 2. If we sort all the verification samples from small to large according to the probability, then $rank_i$ represents the serial number of the positive sample.

Results

Figures 8(a) and (e) show the two original fabric images with different defects, where the defect in (a) is Double Pick and the defect in (e) is Broken End/Warp. The original images appear fuzzy due to the consideration of computation cost. The second and fourth columns show the image histogram before and after the enhancement, where (b) and (f) are the histogram of the original image, (d) and (h) are the histogram of the image after enhancement using the proposed method and (j) and (l) are the histograms of the image after enhancement using grayscale stretching. Figures 8(c), (g), (i) and (k) show the processed image. The results show significant improvement in image sharpness, which makes the defects easy to spot.

Table 2. Definition of *TP*, *FN*, *FP* and *TN* in fabric defect detection

	Detected as defective	Detected as defect-free
Actually defective	True positive (*TP*)	False negative (*FN*)
Actually defect-free	False positive (*FP*)	True negative (*TN*)

After training of local prediction model, we first test the performance of the model on the testing set. The results are shown in Table 3. For the defect prediction task (bi-categorization task), the deep learning-based framework can achieve a significant level with the AUC of 0.912, F_R of 5.7%, D_R of 92.1% and D_{ACC} of 93.2%. The data in second and third columns demonstrate that the proposed enhancement approach can

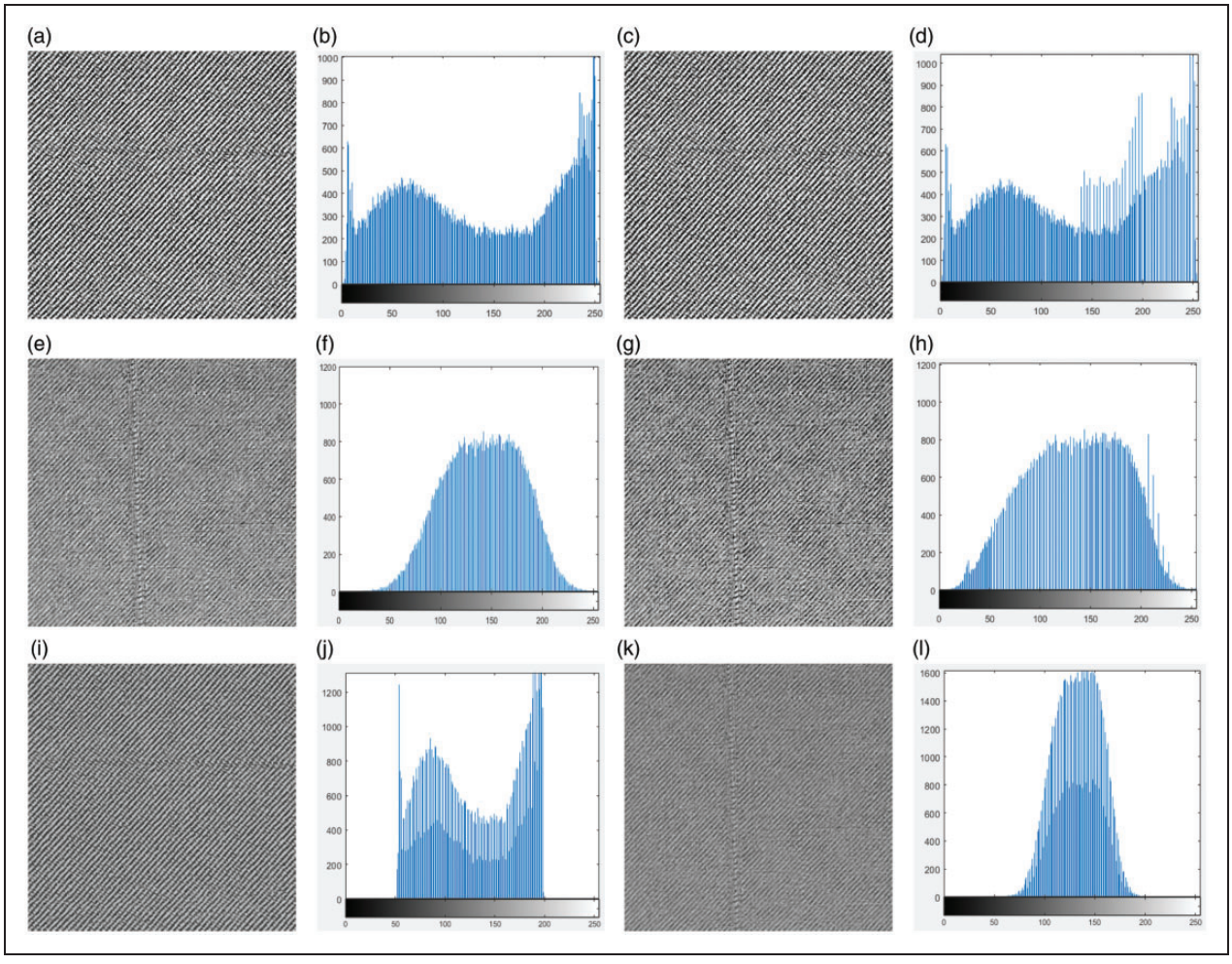

Figure 8. The results of fabric image equalization.

Table 3. The results of the proposed local defect prediction model

Metrics	Without pre-processing	With grayscale stretching	With proposed equalization
Precision			
Normal	92.5%	92.7%	93.7%
No direction	93.3%	93.5%	93.8%
Warp direction	88.6%	91.1%	91.7%
Weft direction	87.6%	89.2%	90.4%
AUC	0.895	0.907	0.912
D_R	90.8%	91.2%	92.1%
F_R	8.6%	6.9%	5.7%
D_{ACC}	91.1%	92.5%	93.2%

improve the performance of defect prediction, especially for warp-direction and weft-direction defects.

For an input image, a series of possibilities are generated, which constitute a feature map. Figure 9 shows three sample images and their feature maps, where the first column is the original images with different defects, the second column is the enlarged images of the defect portion and the third column is the corresponding feature maps. At this scale, it is difficult to find the defects by observing the original images with the human eye. However, from the partially enlarged images we can easily detect the existence of defects. The feature map reflects the distribution of the possibility in the original image. By recognizing the feature map, we can obtain the type of defect in the input image.

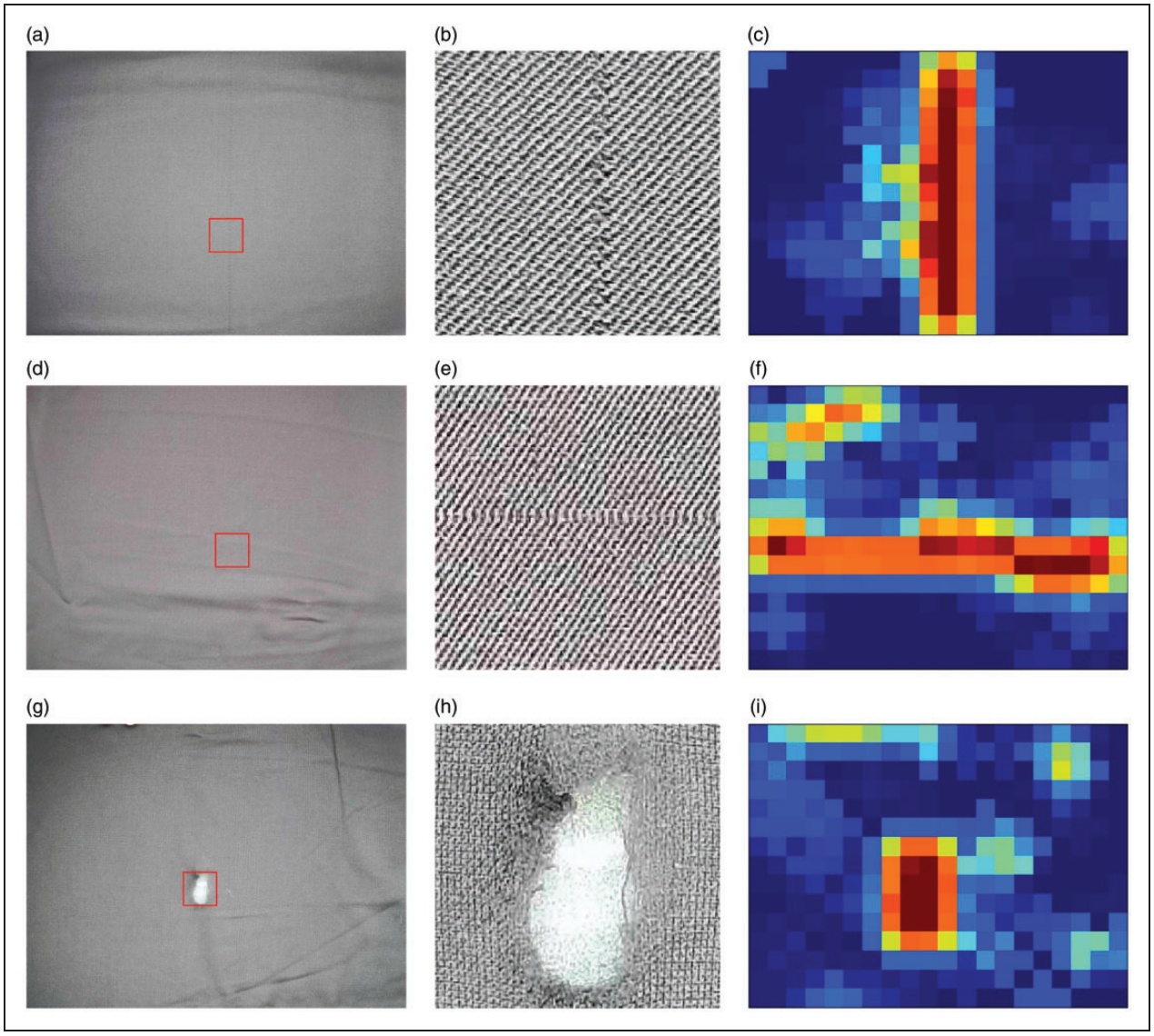

Figure 9. The results of the local defect prediction model.

Due to the significant performance of the local prediction model, the global recognition model achieves a good performance. The role of this model is equivalent to a voting model. Each value in the feature map can be considered as the weight of a vote. The trained classification model reaches an accuracy of 96%. The evaluation metrics of each category are shown in Table 4. We can see that the proposed model has a good performance for all types of defects. Since defects with no direction are more visually significant, the proposed method gains the best score in this category.

Table 4. The recognition result of the proposed model on each classification

	No direction	Warp direction	Weft direction	Total
AUC	0.92	0.91	0.89	0.91
D_R	99%	95%	96%	97%
F_R	5%	7%	6%	6%
D_{ACC}	97%	94%	95%	96%

Table 5. Comparison of recognition results of different prediction models

Models	*AUC*	D_R	F_R	D_{ACC}	Time/s
AlexNet	0.86	92%	7%	93%	2.1
VGG-16	0.9	96%	5%	96%	3.7
Inception-V1	0.91	97%	6%	96%	1.6
Inception-V2	0.91	97%	5%	96%	2.9
Inception-V3	0.93	98%	5%	97%	3.5
ResNet-50	0.92	98%	6%	96%	3.4

Comparisons

Since defect prediction is crucial to defect recognition, this study compares the evaluation metrics from different CNNs, as follows. (1) AlexNet,[7] which is one of the most famous deep learning models, turns CNNs into a core algorithm model for image classification. AlexNet puts more emphasis on the role of the fully connected layer, so two fully connected layers are used in the model. To reduce the computational cost, the author added a dropout layer. (2) VGG-16,[32] which is one of the most influential network structures. It demonstrates the idea that CNNs must rely on deep enough depth to make hierarchical representations of visual data work. (3) Inception-V1[30] (proposed model), (4) Inception-V2[33] and (5) Inception-V3,[31] which are presented by Google. These models are all based on a sparse network module named Inception, which greatly reduces the number of parameters and calculations in CNNs. (6) ResNet-50,[34] which is currently the most popular deep learning model. ResNet uses a ''jump connection'' to avoid gradient disappearance and degradation problems caused by the network being too deep. The experimental results are shown in Table 5. All six networks have a good performance on the proposed dataset. The results demonstrate that the deep learning-based method is a good choice for the task of fabric defect detection. However, considering the difference in computational cost, Inception-V1 achieves the same level in less time. This is the reason why Inception-V1 is proposed in this paper.

To further validate the effectiveness of the proposed framework in fabric detection, we compare the performance of the proposed method with the other five representation defect detection models, as follows. (1) The differential evolution-based optimal Gabor filter model (DEP),[35] which is one of the most popular methods for fabric defect detection, and has shown superior performance on fabric defect inspection compared with

Table 6. Comparison of recognition results of different defect detection methods

	Total testing set					Testing set with small defects and folds			
	AUC	D_R	F_R	D_{ACC}	Time/s	*AUC*	D_R	F_R	D_{ACC}
DEP	0.82	86%	13%	87%	0.4	0.71	79%	24%	77%
GB	0.71	79%	18%	81%	0.3	0.68	74%	28%	72%
AS	0.83	88%	14%	87%	0.6	0.74	78%	25%	75%
FW	0.78	85%	12%	86%	0.6	0.74	76%	24%	77%
DL	0.85	90%	9%	91%	0.8	0.79	81%	19%	81%
Proposed	0.91	97%	5%	96%	1.6	0.87	92%	10%	90%

DEP: differential evolution-based optimal Gabor filter model; GB: Gabor filter bank-based model; AS: adaptive sparse representation-based model; FW: Fourier and wavelet shrinkage-based model; DL: dictionary learning-based model.

some classical fabric detection models in terms of detection accuracy computational cost. The DEP performs well in detecting linear fabric defects, such as defects in the weft direction and warp direction, because the Gabor filters applied in this model are optimized in the horizontal and vertical directions. (2) The Gabor filter bank-based model (GB),[2] which is widely considered as a classical method for fabric detection and is a supervised approach. (3) The adaptive sparse representation-based model (AS),[36] which is an effective method that utilizes image noise reduction techniques. (4) The Fourier and wavelet shrinkage-based model (FW),[37] which is one of the latest spectrum-based methods for fabric defect detection. (5) The dictionary learning-based model (DL),[27] which is based on non-locally centralized sparse representation. The DL mainly applies two modules: dictionary learning and fabric defect detection through image restoration.

The comparative results on our dataset are shown in Table 6. The DEP model by using Gabor filters heavily depends on feature extraction, which lead to the limitations of the detection method. The GB model is sensitive to some small texture variations, which lead to the high false alarm rate. In addition, these learning-based methods (DL and proposed) perform much better on our datasets than others. The proposed method is significantly better than DL in terms of detection accuracy, but it is a significant disadvantage in terms of time consuming. However, the false alarm rate of proposed method is much lower than other methods. Moreover, the higher AUC of the proposed method indicates that the method is more accurate in identifying defects. Moreover, we specifically selected fabrics with small defects (the length and width of the area where the defect is located are not greater than 10 pixels) and folds to form a test data set with 152 samples. Then we conducted a comparative experiment on this data set, and the results showed that (1) the proposed also has good performance in detecting small defects; (2) the proposed model can distinguish between defects and folds. In summaries, the proposed framework, which is based on deep learning, have a stronger adaptability to different defects.

Conclusion

In this paper, we present an effective deep learning-based framework, which aims to detect defects in the fabric. Firstly, an efficient HE is used to enhance the fabric image. Then we apply a CNN, which is based on a sparse network structure named Inception to predict the existence of defects in the local area. After the prediction, a feature map corresponding to the input image is formed. Finally, the LeNet-5 model is employed to vote and recognize the defect. Experimental results demonstrate the superiority of the proposed framework.

Compared with traditional methods, the disadvantages of those methods, which are based on deep learning, are the large computational cost and time consumption. So, the current challenge of this study is how to minimize detection time while maintaining high accuracy. In addition, this study simply divided fabric defects into three categories (no-direction defects, warp-direction defects and weft-direction defects), including most types of defects. Indeed, the proposed algorithm can only roughly identify fabric defects, so that it is difficult to accurately output the reason for the defects. With the accumulation of data, we will continue to study how to accurately identify the defect classification used in the factory in the subsequent research.

Declaration of conflicting interests

The author(s) declared no potential conflicts of interest with respect to the research, authorship, and/or publication of this article.

Funding

The authors received no financial support for the research, authorship and/or publication of this article.

ORCID iD

Jun Xiang https://orcid.org/0000-0001-5177-0812

References

1. Kumar A. Computer-vision-based fabric defect detection: a survey. *IEEE Trans Ind Electron* 2008; 55: 348–363.
2. Kumar A and Pang GK. Defect detection in textured materials using Gabor filters. *IEEE Trans Ind Appl* 2002; 38: 425–440.
3. Shady E, Gowayed Y, Abouiiana M, et al. Detection and classification of defects in knitted fabric structures. *Text Res J* 2006; 76: 295–300.
4. Zhang YF and Bresee RR. Fabric defect detection and classification using image analysis. *Text Res J* 1995; 65: 1–9.
5. Chan C-h and Pang GK. Fabric defect detection by Fourier analysis. *IEEE Trans Ind Appl* 2000; 36: 1267–1276.
6. Kim S, Lee MH and Woo K-B. Wavelet analysis to fabric defects detection in weaving processes. In: *proceedings of the IEEE international symposium on industrial electronics (ISIE'99) (Cat. No. 99TH8465)*, Bled, Slovenia, 12–16 July 1999, pp.1406–1409. Washington, DC: IEEE.
7. Krizhevsky A, Sutskever I and Hinton G. ImageNet classification with deep convolutional neural networks. In: *international conference on neural information processing systems*, (eds F. Pereira, C.J.C. Burges, L. Bottou and K.Q. Weinberger), Lake Tahoe, Nevada, United States,

3–6 December 2012, pp.1097–1105. New York, United States: Curran Associates Inc.
8. LeCun Y, Bengio Y and Hinton G. Deep learning. *Nature* 2015; 521: 436.
9. Schmidhuber J. Deep learning in neural networks: an overview. *Neural Network* 2015; 61: 85–117.
10. Deng L and Yu D. Deep learning: methods and applications. *Foundat Trend Sign Proc* 2014; 7: 197–387.
11. Mnih V, et al. Playing Atari with deep reinforcement learning. *arXiv preprint arXiv:1312.5602*2013.
12. Andrearczyk V and Whelan PF. Using filter banks in convolutional neural networks for texture classification. *Patt Recognit Lett* 2016; 84: 63–69.
13. Liu L, Chen J, Fieguth P, et al. From BoW to CNN: two decades of texture representation for texture classification. *Int J Comput Vis* 2019; 127: 74–109.
14. Andrearczyk V and Whelan PF. Convolutional neural network on three orthogonal planes for dynamic texture classification. *Patt Recognit* 2018; 76: 36–49.
15. Bu H-g, Wang J and Huang X-b. Fabric defect detection based on multiple fractal features and support vector data description. *Eng Appl Artif Intell* 2009; 22: 224–235.
16. Mak K, Peng P and Lau H. Optimal morphological filter design for fabric defect detection. In: *2005 IEEE international conference on industrial technology*, Hong Kong, China, 14–17 December 2005, pp.799–804. New York: IEEE.
17. Mak K-L, Peng P and Yiu KFC. Fabric defect detection using morphological filters. *Image Vis Comput* 2009; 27: 1585–1592.
18. Zhu D, Pan R, Gao W, et al. Yarn-dyed fabric defect detection based on autocorrelation function and GLCM. *Autex Res J* 2015; 15: 226–232.
19. Zhang K, Yan Y, Li P, et al. Fabric defect detection using salience metric for color dissimilarity and positional aggregation. *IEEE Access* 2018; 6: 49170–49181.
20. Lambert G and Bock F. Wavelet methods for texture defect detection. In: *proceedings of international conference on image processing*, 1997, Santa Barbara, CA, USA, 26–29 October 1997, vol. 3, pp.201–204. Washington, DC: IEEE.
21. Bodnarova A, Bennamoun M and Latham S. Optimal Gabor filters for textile flaw detection. *Patt Recognit* 2002; 35: 2973–2991.
22. Jia L, Chen C, Liang J, et al. Fabric defect inspection based on lattice segmentation and Gabor filtering. *Neurocomputing* 2017; 238: 84–102.
23. Xiaobo Y. Fabric defect detection of statistic aberration feature based on GMRF model. *J Text Res* 2013; 4: 026.
24. Allili MS, Baaziz N and Mejri M. Texture modeling using contourlets and finite mixtures of generalized Gaussian distributions and applications. *IEEE Trans Multimedia* 2014; 16: 772–784.
25. Kumar A. Neural network based detection of local textile defects. *Patt Recognit* 2003; 36: 1645–1659.
26. Kuo C-FJ, Lee C-J and Tsai C-C. Using a neural network to identify fabric defects in dynamic cloth inspection. *Text Res J* 2003; 73: 238–244.
27. Tong L, Wong WK and Kwong C. Fabric defect detection for apparel industry: a nonlocal sparse representation approach. *IEEE Access* 2017; 5: 5947–5964.
28. Ouyang W, Xu B, Hou J, et al. Fabric defect detection using activation layer embedded convolutional neural network. *IEEE Access* 2019; 7: 70130–70140.
29. Li C, Gao G, Liu Z, et al. Fabric defect detection based on biological vision modeling. *IEEE Access* 2018; 6: 27659–27670.
30. Szegedy C, et al. Going deeper with convolutions. In: *proceedings of the IEEE conference on computer vision and pattern recognition*, (eds K. Grauman and E.K. Miller and A.Torralba), Massachusetts, Boston, United States, 8-10 June 2015, pp.1–9. Washington, DC: IEEE.
31. Szegedy C, Vanhoucke V, Ioffe S, et al. Rethinking the inception architecture for computer vision. In: *proceedings of the IEEE conference on computer vision and pattern recognition*, Las Vegas, United States, 26 June–1 July 2016, pp.2818–2826. Washington, DC: IEEE.
32. Simonyan K and Zisserman A. Very deep convolutional networks for large-scale image recognition. *Comput Sci* 2014; arXiv preprint arXiv:1409.1556.
33. Ioffe S and Szegedy C. Batch normalization: accelerating deep network training by reducing internal covariate shift. *arXiv preprint arXiv:1502.03167*2015.
34. He K, Zhang X, Ren S, et al. Deep residual learning for image recognition. In: *proceedings of the IEEE conference on computer vision and pattern recognition*, Las Vegas, United States, 26 June–1 July 2016, pp.770–778. Washington, DC: IEEE.
35. Tong L, Wong WK and Kwong C. Differential evolution-based optimal Gabor filter model for fabric inspection. *Neurocomputing* 2016; 173: 1386–1401.
36. Zhou J and Wang J. Fabric defect detection using adaptive dictionaries. *Text Res J* 2013; 83: 1846–1859.
37. Hu G-H, Wang Q-H and Zhang G-H. Unsupervised defect detection in textiles based on Fourier analysis and wavelet shrinkage. *Appl Opt* 2015; 54: 2963–2980.